Chemical Engineering Journal 154 (2009) 107–114

Contents lists available at ScienceDirect

Chemical Engineering Journal

journal homepage: www.elsevier.com/locate/cej

The simplest self-assembled monolayer model with different orientations of complex organic molecules. Monte Carlo and transfer-matrix techniques

V.F. Fefelov[a], V.A. Gorbunov[a,*], A.V. Myshlyavtsev[a,b], M.D. Myshlyavtseva[a]

[a] Omsk State Technical University, Omsk, Russia
[b] Institute of Hydrocarbons Processing SB RAS, Omsk, Russia

ARTICLE INFO

Article history:
Received 10 December 2008
Received in revised form 19 March 2009
Accepted 13 April 2009

Keywords:
Self-assembled monolayer
Adsorption
Monte Carlo simulation
Transfer-matrix method

ABSTRACT

In the present paper we construct and study the simplest model of self-assembled monolayer (SAM) with several different orientations of complicated organic molecules with respect to the interface. In order to study the model we used transfer-matrix and Monte Carlo techniques. It was shown that the structures of the model ordered phases are analogous to the structures of real SAMs. Our model of SAMs demonstrates the non-monotonous dependence of the total coverage versus pressure (chemical potential), i.e. at the increase of pressure the empty surface area can grow that can take some effect on physicochemical processes on surface.

1. Introduction

Self-assembled monolayers (SAMs) of complicated organic molecules can be formed on the solid/gas [1], solid/liquid [2], or liquid/gas [3] interfaces. SAMs have numerous applications for thin films containing these materials including gas sensing, catalysis, light emitting diodes, nonlinear optics, molecular-based information storage, coating for the protection of surfaces from corrosion and so on [1–4]. For example the aromatic molecule p-Sexiphenil (p-6P) has been used in the active layer of an organic blue-light-emitting diode [1]. One of the most interesting features of these systems is the possibility of two or more different orientations of complicated organic molecules with respect to the interface [1–3,5,6]. The possible orientation depends on concentration, pressure, temperature, surface electric potential and other parameters. It should be noticed that there are the ordered structures which contains the molecules with two different orientations (for example—p-Sexiphenil on the Au(1 1 1) surface in ultrahigh vacuum) [1]. Existence of several molecule orientations with respect to the interface results in the dependence of the average interface area per molecule on the pressure or other parameters. As an example we can refer to [3], where the surface pressure–area isotherms (area per molecule versus surface pressure curves) of tetrapyridylporphyrin monolayers on pure water and water solutions containing Cd^{2+} or Cu^{2+} were obtained. It was shown that molecule area decreases with the growth of surface pressure.

The goal of presented work is the construction and study of the simplest SAMs model with several orientations of complicated organic molecules with respect to the interface. We elaborated the model with several ordered structures including the structure with two types of molecule orientations. It should be noticed that at present time the theoretical study of the monolayers of the complicated linear [7–14] or nonlinear [4,9,10,15–17] molecules is in the very beginning.

2. Model

It is well known that a lattice gas model is a very good approximation for chemisorptions [18–20], and we consider the one as the SAMs model. The simplest model with two different molecule orientations with respect to surface have been recently studied [7,14]. This model is the dimer model with two possible orientations with respect to surface: in parallel occupying the two nearest active centers and transversally occupying the only one. It should be noticed that in the framework of the model the direct proportionality between the surface coverage and the number of adsorbed particles is broken.

The molecules adsorbed by the various ways can be differed by their adsorption heats naturally. The different lateral interactions between the adsorbed particles can be included in the model as well.

As it was shown the presented model [14] demonstrates the rich and non-trivial phase diagram. Let us describe qualitatively

* Corresponding author.
E-mail addresses: fefelov_vasiliy@mail.ru (V.F. Fefelov), vitaly_gorbunov@mail.ru (V.A. Gorbunov), myshl@omgtu.ru (A.V. Myshlyavtsev).

1385-8947/$ – see front matter © 2009 Elsevier B.V. All rights reserved.
doi:10.1016/j.cej.2009.04.036

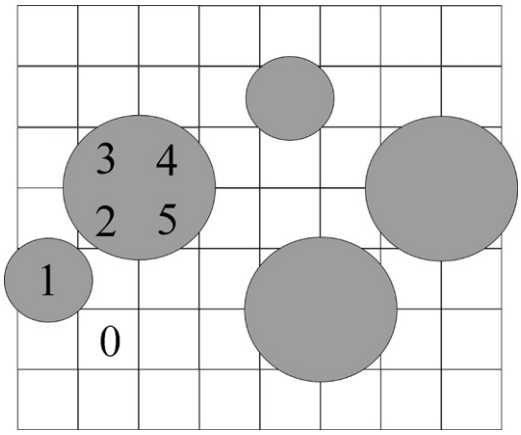

Fig. 1. The allowed configurations of the adsorbed particles. The small circles denote the mono-center adsorbed particles and the large circles denote the four-center adsorbed particles. The numbers from 0 up to 5 denote all of the possible states of the lattice cells.

the surface filling by the adsorbed particles with the pressure increasing. We also assume that the adsorption heat at parallel location is larger than that at perpendicular one. For model under consideration the surface filling takes place in the following way. At the beginning at low pressures the most of the adsorbed particles are placed in parallel with the surface. On the increase of the gas phase pressure the molecules adsorbed transversally to the surface begin to occur. Their portion gradually increases and the portion of the molecules adsorbed in parallel to the surface begins to decrease. Finally, at the high pressures the most of the adsorbed particles are placed transversally to the surface. Obviously, when the described scenario is realized the direct proportionality between the number of adsorbed molecules and the surface coverage is absent. However, as the numerical results display, in the framework of this model the dependence of the surface coverage on the pressure is monotonic as before. Let us generalize the considered model of the dimer adsorption and elaborate the lattice gas model for adsorption of the complicated molecules. We assume the molecule can be adsorbed on the surface by the k ways occupying the m_1, m_2, ..., m_k active centers located in the corresponding configurations on homogeneous or heterogeneous lattice, respectively. One of the simplest models of this type (not counting the described model of the dimer adsorption) is as follows.

We consider the homogeneous square lattice as the surface model and assume that the molecules can be adsorbed by only two different ways. At the first way the molecule occupies the one active center and at the second way the molecule does the four ones. These four centers form the square. Thus, for our model we have $k = 2$, $m_1 = 1$, $m_2 = 4$. We assume that a nearest neighborhood between two adsorbed molecules (independently of the adsorption way) is prohibited as well. The allowed configurations of the adsorbed particles are schematically shown in Fig. 1. The difference between the heats of adsorption of the four-center location and the mono-center one is noted as Δ. At positive value of Δ the sequence of the surface filling by the adsorbate is quite analogous to that in the case of the dimer adsorption. Evidently, as in the case of the dimer adsorption models the proportionality between the number of adsorbed particles and the surface coverage is absent. Thermodynamic Hamiltonian for the model under consideration can be written as

$$H = \frac{\Delta}{4}\sum_i n_i + \mu\left(\frac{1}{4}\sum_i n_i + \sum_i c_i\right), \quad (1)$$

where the occupation numbers c_i and n_i are equal to unity for occupied by molecule adsorbed on one and four sites respectively and zero for empty sites; μ is the chemical potential of the adsorbed particles.

3. Phase diagram in the ground state

For model under consideration we can easily obtain the exact phase diagram in the (μ, Δ) plane in the ground state (i.e. at $T = 0$). At these conditions total energy for any ordered phase can be calculated from the Hamiltonian directly since each ordered phase is characterized by specific symmetry properties which determine the arrangement of differently oriented molecules over the surface. In this case stability of each phase is determined by minimum of total energy of the system at given value of chemical potential.

As we assume all the nearest-neighbor interactions are infinite repulsive the model predicts the following ordered structures with different densities: $c(4\times4)_4$, $c(3\times3)_{4-1}$, $c(2\times2)$ being schematically shown in Fig. 2. Moreover, there exists a gas phase which has got the energy equal to zero in the ground state.

Let us consider the cluster consisting of 12×12 sites. This size of cluster is a minimal lattice size on which all elementary structures of appearing phases are packed. Assuming $(-\Delta\ -\mu)$ as adsorption energy per molecule with $m_2 = 4$ and $(-\mu)$ adsorption energy for molecule with $m_1 = 1$ the total energy according to each above ordered structure (see Fig. 2) is equal:

$$\Omega_1 = 0, \quad (2)$$

$$\Omega_2 = -18\Delta - 18\mu, \quad (3)$$

$$\Omega_3 = -16\Delta - 32\mu, \quad (4)$$

$$\Omega_4 = -72\mu, \quad (5)$$

where Ω_1 is total energy for empty lattice (lattice gas (LG)); Ω_2, Ω_3 and Ω_4 is total energy for the structures $c(4\times4)_4$, $c(3\times3)_{4-1}$ and $c(2\times2)$ respectively.

The existence condition for LG is $\Omega_1 < \Omega_2$. In terms of expressions (2) and (3) this condition can be written as:

$$\mu < -\Delta \quad (6)$$

Analogically, we obtain $\mu < 1/7\Delta$ the existence condition for the structure $c(4\times4)_4$, $c(3\times3)_{4-1}$ and $c(2\times2)$:

$$\mu < \frac{1}{7}\Delta, \quad (7)$$

$$\mu < \frac{2}{5}\Delta, \quad (8)$$

and

$$\mu > \frac{2}{5}\Delta \quad (9)$$

respectively. Thus, we build phase diagram for the system considered in the ground state (Fig. 3).

4. Methods

The calculation of the isotherms, the surface coverage or the phase diagrams as the function of the gas phase pressure (chemical potential) is a rather difficult problem for the model under consideration. In general, the two-dimensional multi-center adsorption model for which the exact analytic solution can be obtained does not exist. For the mono-center adsorption that model is well known Langmuir model of adsorbed overlayer [18–21]. Thus we should use one of the approximate methods suitable for our purposes. The most suitable techniques for our model are the well known in the field of the modern theoretical physics transfer-matrix method (TMM) and Monte Carlo method.

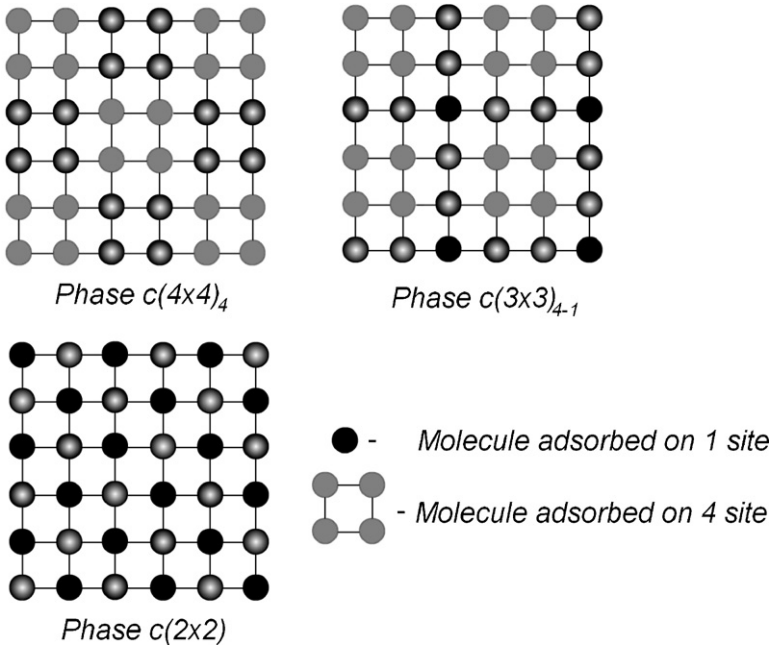

Fig. 2. Ordered structures of adlayer.

4.1. Transfer-matrix technique

The heart of this method is to replace the difficult problem of the grand partition function calculation for the two-dimensional lattice model by the simpler problem of calculation of the largest magnitude eigenvalue and the eigenvector corresponding to this eigenvalue for some matrix [22–27]. In the framework of this technique the two-dimensional lattice is replaced by the strip that is infinite in one direction and has finite width M in the perpendicular direction. TMM gives the exact values of the grand partition function for this semi-infinite system. Obviously, with the increasing M the calculated quantities tend to the exact values for the infinite two-dimensional lattice. Note that the local quantities such as isotherms are dependent on the nearest environment and independent of whether or not there is long range order. Therefore, using even relatively small M values it is possible to yield practically exact results. For our model the each cell can be in six states marked by the numbers 0–5 in Fig. 1. The calculations have been carried out with the value $M = 12$. As it is going to show below, we must use values M which are a multiple of twelve, however, already the value $M = 24$ was too large for our computer resources. The transfer-matrix can be written in the following form

$$\mathbf{T} = \mathbf{DAD}, \tag{10}$$

where $\mathbf{D}$ is a diagonal matrix. For the model under consideration a central matrix $\mathbf{A}$ can be represented as a M-fold tensor product

$$\mathbf{A} = \underbrace{\mathbf{t} \otimes \mathbf{t} \otimes \mathbf{t} \otimes \ldots \otimes \mathbf{t} \otimes \mathbf{t}}_{M}, \tag{11}$$

where $\mathbf{t}$ is a 6×6 matrix. The latter expression allows to construct a very effective numerical algorithm [26] for calculation of the largest magnitude eigenvalue and the eigenvector corresponding to this eigenvalue.

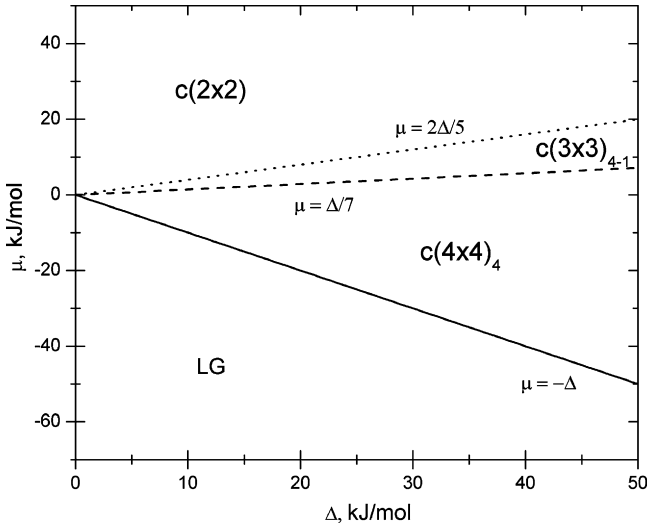

Fig. 3. Ground state phase diagram for the model. The solid line separates the regions of stability of LG and $c(4 \times 4)_4$ ordered phase, while dash line and dot line separate the regions of stability of the phases $c(4 \times 4)_4$–$c(3 \times 3)_{4-1}$ and $c(3 \times 3)_{4-1}$–$c(2 \times 2)$, respectively.

4.2. Monte Carlo simulation scheme

The thermodynamic properties of the model have been investigated with standard importance sampling Monte Carlo method [27]. Square lattice of $M = L \times L$ size with periodic boundary conditions is considered as surface model. Note the linear lattice size is chosen for the adlayer structures to be not perturbed. Calculations are carried out with the values $L = 96$ and $L = 24$; 36; 48; 60 for the simulation of isotherms and for finite-size scaling procedures, respectively. Thermodynamic equilibrium is reached by spin-flip (Glauber) dynamics and diffusion relaxation (Kawasaki dynamics). To simulate adsorption isotherms successive configurations of the adlayer are generated using Metropolis transition probabilities [28] in the grand canonical ensemble. For a given value of μ and T the initial configuration is generated. Any change in overlayer structure has been accepted with unit probability if it resulted in the decrease the system energy and, otherwise, has been rejected if $r > \exp(-dH/k_BT)$, where r is random number such that $0 < r < 1$. The Hamiltonian difference of such change is dH.

The first 10^6 Monte Carlo steps (MCS) of each run had been performed to establish the equilibrium and the next 10^6 MCSs were used to compute averages. However, in the vicinity of critical points up to 10^7 MCS had to be used because fluctuations are greatly enhanced. Note, one Monte Carlo step corresponds to one run over the entire lattice.

Thermodynamic quantities such as (12) amount of spaces adsorbed on the lattice (density) $\rho(\mu)$; (13) coverage by molecules adsorbed on 1 site $\theta_1(\mu)$; (14) coverage by molecules adsorbed on 4 site $\theta_4(\mu)$; and (15) total coverage of the lattice $\theta(\mu)$ are obtained as simple averages:

$$\rho(\mu) = \frac{1}{M}\left(\frac{1}{4}\sum_i n_i + \sum_i c_i\right), \tag{12}$$

$$\theta_1(\mu) = \frac{1}{M}\sum_i c_i, \tag{13}$$

$$\theta_4(\mu) = \frac{1}{M}\sum_i n_i, \tag{14}$$

$$\theta(\mu) = \theta_1(\mu) + \theta_4(\mu). \tag{15}$$

Error bars for these values are given by

$$\sigma = \sqrt{(\langle A^2\rangle - \langle A\rangle^2)\left(\frac{2\tau_A}{t}\right)}, \tag{16}$$

where A is the value of interest; τ_A is correlation time for A and t is observation time. In order to determine the correlation time we calculated the normalized time autocorrelation function

$$\phi_A(t) = \frac{\langle A(0)A(t)\rangle - \langle A\rangle^2}{\langle A^2\rangle - \langle A\rangle^2} \tag{17}$$

and then we interpreted the correlation time as time integral of $\phi_A(t)$ [27]

$$\tau_A = \int_0^\infty \phi_A(t)dt. \tag{18}$$

The coverage θ is the usual order parameter in the presence of a first-order phase transition; however, it does not apply to ordered structures. In that case, it is convenient to consider the possible structure of adlayer and related order parameter φ. Let us define order parameter for $c(4\times4)_4$ phase (Fig. 2). Due to the periodic boundary conditions the degeneracy of this phase depending on location of left top segment of the molecule adsorbed on 4 sites (segment pointed as "3" on Fig. 1) is equal to 16. These configurations allow us to decompose the original lattice in such specific way that all ordered configurations of the phase put into eight different sublattices (see Fig. 4). The coverage on each sublattice is denoted as θ_i. In such considerations, order parameter for the phase $c(4\times4)_4$ can be defined as

$$\varphi_{4\times4} = |\theta_1 - \theta_2| + |\theta_3 - \theta_4| + |\theta_5 - \theta_6| + |\theta_7 - \theta_8|, \tag{19}$$

where sum the differences (in absolute value) between the coverage corresponding to two complementary sublattices. When the system is disordered all sublattices are equivalent and the order parameter is minimal. However, when $c(4\times4)_4$ structure appears all left top segments of the molecule adsorbed on 4 sites are allocated in one sublattice. That is the coverage of this sublattice (θ_i) is maximal ($\theta_i = 1$) and the coverage of the complementary sublattice is zero. In addition, the rest of the sum is zero or minimum. Thus, order parameter $\varphi_{4\times4}$ is convenient for defining of order–disorder phase transition.

Other appearing phase is $c(3\times3)_{4-1}$ phase consisting with molecules adsorbed on 4 and 1 sites, simultaneously. The degeneracy of this configuration equals to 9, so we should separate the original lattice into nine different sublattices (Fig. 5). To calculate the coverage of the given sublattice we have to assume that $\theta_i = \theta_i^1 + \theta_i^2$, where θ_i^1 denotes coverage of part of sublattice assumed for only left top segment of the molecule adsorbed on 4 sites. On the other hand, θ_i^2 is coverage of that part of sublattice assumed only for on top adsorbed molecule. Further, the sublattice with maximum coverage is determined, and the order parameter can be calculated as

$$\varphi_{3\times3} = \theta_{i,\max} - \frac{1}{8}\sum_{j,j\neq i}\theta_j. \tag{20}$$

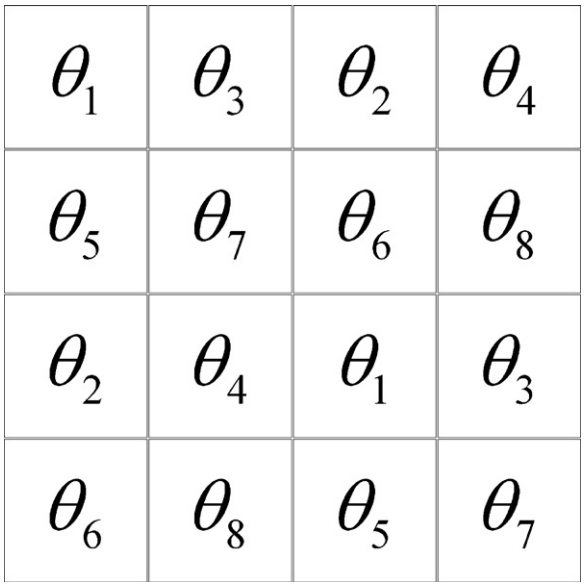

Fig. 4. Sublattices for calculating of order parameter $\varphi_{4\times4}$. θ_i is coverage of each sublattice depending on the location of left top segment of the molecule adsorbed on 4 sites.

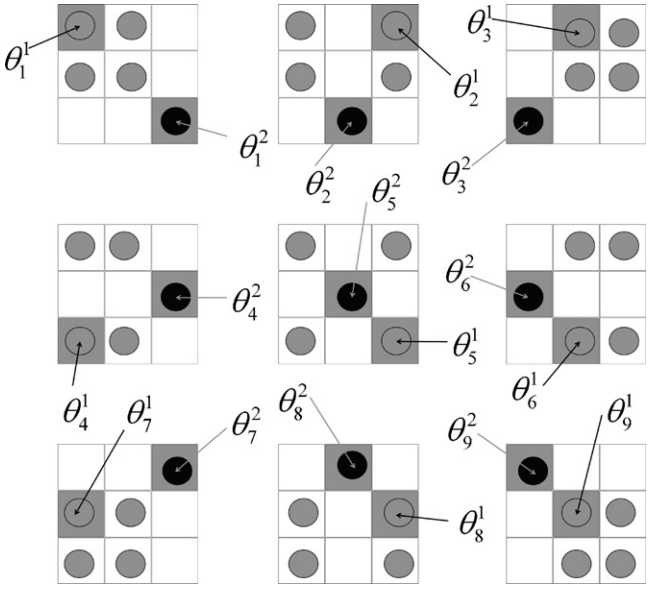

Fig. 5. All possible sublattices for calculating of order parameter $\varphi_{3\times3}$. θ_i^1 denotes coverage of part of sublattice assumed for only left top segment of the molecule adsorbed on 4 sites. On the other hand, θ_i^2 is coverage of that part of sublattice assumed only for on top adsorbed molecule.

We define the last $c(2\times2)$ ordered phase in the system with traditional order parameter [19]

$$\varphi_{2\times2} = |\theta_1 - \theta_2| \tag{21}$$

where θ_1 and θ_2—coverage of the corresponding sublattices. Error bars for all order parameters are determined with Eq. (16).

The quantities related to the order parameter, such as the susceptibility χ, and the reduced fourth-order cumulant U_L introduced by Binder [27,29], can be calculated as:

$$\chi = \frac{L^2(\langle\varphi^2\rangle - \langle\varphi\rangle^2)}{T}, \tag{22}$$

$$U_L = 1 - \frac{\langle\varphi^4\rangle}{3\langle\varphi^2\rangle^2}. \tag{23}$$

According to the standard finite-size scaling theory the order–disorder transition in a finite system is rounded and shifted in contrast to infinite system at $M\to\infty$, so the transition parameters should be determined from suitable scaling relationships [27]. One of the them relies on the extrapolation of the positions $T_c(L)$ (or $\mu_c(L)$) of the susceptibility maxima $\chi(T)_{\max}$ (or $\chi(\mu)_{\max}$). For this quantity one expects

$$\mu_c(L) = \mu_c(\infty) + \text{const}\cdot L^{-1/\nu},\ L\to\infty, \tag{24}$$

where ν is standard critical exponent of correlation length.

Other possible route to estimate the true transition temperature (or chemical potential) can be determined from the plots $U_L(T)$ (or $U_L(\mu)$) obtained for various values of L, because all such curves have an intersection point at T_c (or μ_c) and the fixed value U_φ^*. The value U_φ^* characterizes the universality class of a transition. The critical exponents can be evaluated by using the well known finite-size scaling techniques [27,30].

In case of susceptibility and Binder's fourth-order cumulant it is not possible to estimate the error in value using the direct method (Eq. (16)). Therefore, we used the bootstrap method [35].

The multiple-histogram reweighting [31–34] was applied to estimate first-order phase transitions. The coexisting curves were determined according to a "two-state approximation" from the density distribution [33,34]

$$p(\rho) = \sum_u P(\rho, u), \tag{25}$$

where u is the potential energy of the system and $P(\rho,u)$ is the two-dimensional histogram. In the case of a first-order transition the density distribution $p(\rho)$ has a double peaked structure. The precise location of a coexistence point is achieved by tuning the chemical potential at a given temperature until the areas under both peaks become the same.

5. Results and discussion

5.1. Isotherms and coverage curves

The set of isotherms for different values of Δ obtained with Monte Carlo (Fig. 6(a)) and transfer-matrix technique (Fig. 6(b)) is shown in Fig. 6. The identity of presented curves indicates that our results are true. Note, we did not show the error bars on Figs. 6–8 because ones are very small and not exceed 2%. There are three evident plateaus appearing at sufficiently high values of Δ in the isotherms. Fig. 7 shows isotherm at $\Delta = 30$ kJ/mol with corresponding ordered structures of adlayer. The steps between the plateaus indicate first-order phase transitions which are characterized by abrupt change of free energy of system. In the considered system it is disclosed by discontinuity of amount of adsorbed spaces $p(\mu)$. Moreover, size of this jump is unimportant in terms of the classification of phase transitions. On the other hand, "'LG-$c(4\times4)_4$" phase transition is typical second order phase transition. In this case at critical point a symmetry element arise in the system, but the amount the adsorbed spaces change continuously.

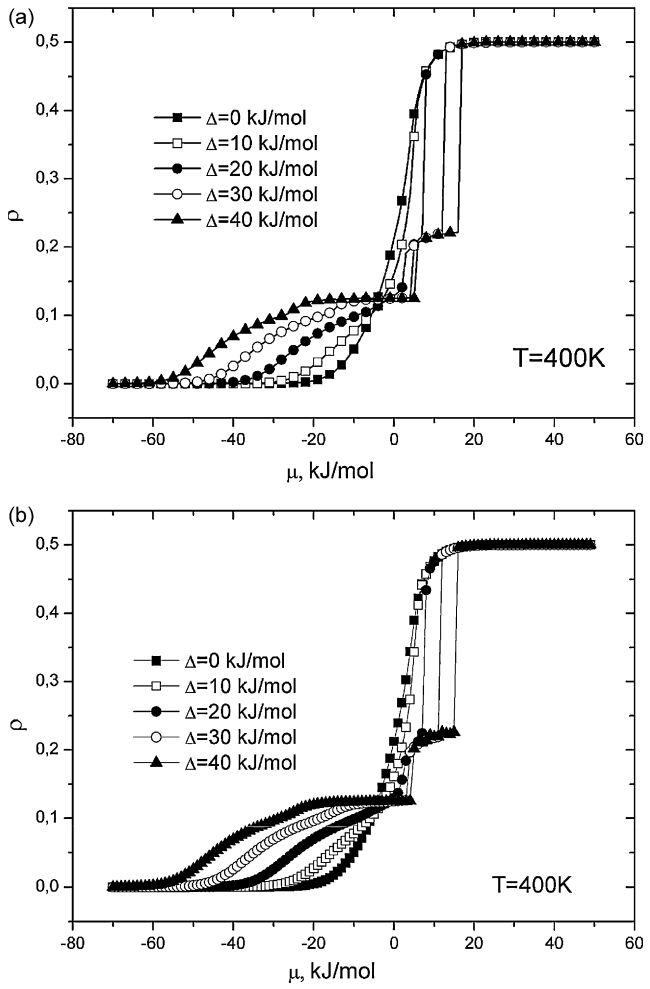

Fig. 6. Set of isotherms for different values of A obtained with Monte Carlo (a) and transfer-matrix technique (b).

This specific phase behavior has simple physical interpretation. At the high values of the Δ it is energetically efficient to adsorb

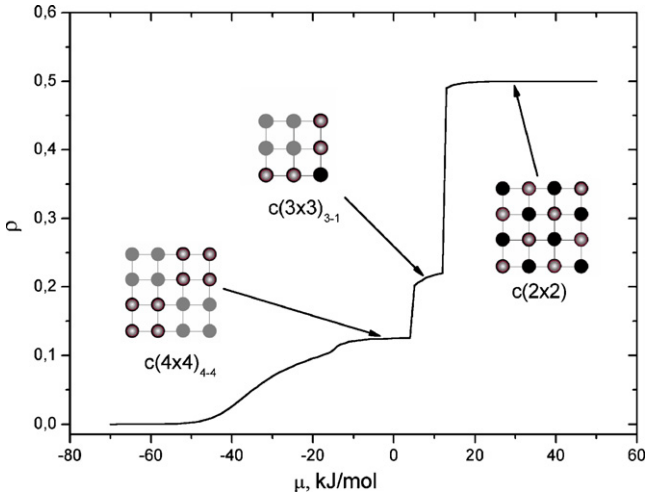

Fig. 7. The isotherm calculated at $T = 400$ K, $\Delta = 30$ kJ/mol with ordered structures.

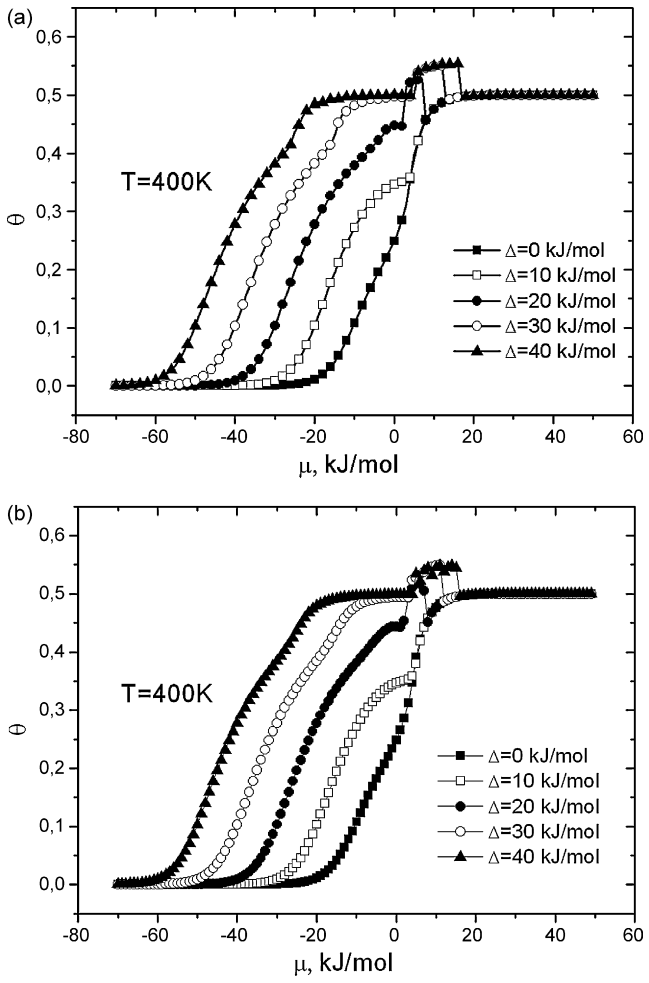

Fig. 8. Coverage versus chemical potential curves for different values A obtained with Monte Carlo (a) and transfer-matrix technique (b).

on four sites. Oppositely, when values Δ are low (0 or 10 kJ/mol) adsorption on four sites is steric complicated.

In the Fig. 8 we presented coverage versus chemical potential curves for different values Δ obtained with Monte Carlo (Fig. 8(a)) and transfer-matrix technique (Fig. 8(b)). One can see that these sets of curves are identical. It points out the reliability of our results. For sufficiently large values of Δ there are three well-defined plateaus on the curves corresponded to above mentioned ordered phases. Each ordered phase has its own coverage: for $c(4\times4)_4$ is $\theta = 0.5$; for $c(3\times3)_{4-1}$–$\theta = 0.55(5)$; for $c(2\times2)$–$\theta = 0.5$. Note, that in the case of ordered phases consisting with molecules with the same orientation in adlayer, $c(4\times4)_4$ and $c(2\times2)$, coverages equal to 0.5. However, complex structure formed by molecules adsorbed as on one as on four adsorption sites ($c(3\times3)_{4-1}$) has the largest coverage $\theta = 5/9$.

It should be marked that the first-order phase transition $c(3\times3)_{4-1}$–$c(2\times2)$ goes with decreasing of coverage. That is the coverage dependence of chemical potential is nonmonotonic. It means when pressure in the gas phase growths the amount of empty adsorption sites growths too. This unusual phenomenon was not reported in literature before. Nonmonotonic changing of coverage is explained by appearing of complex phase $c(3\times3)_{4-1}$.

5.2. Phase diagram

For sufficiently large values of the Δ value the system undergoes the phase transitions. Depending on the temperature region

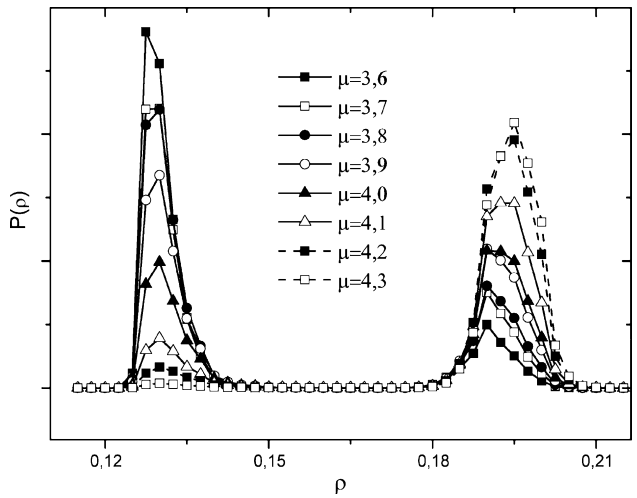

Fig. 9. Density distributions for $T = 500$ K, $\Delta = 30$ kJ/mol and different values of μ at first-order phase transition $c(4\times4)_4$–$c(3\times3)_{4-1}$.

there are two first-order and three second-order phase transition in the adlayer under consideration. The first-order phase transitions take place between all mentioned above ordered structures: $c(4\times4)_4$–$c(3\times3)_{4-1}$ and $c(3\times3)_{4-1}$–$c(2\times2)$ transitions. On the other hand, second-order phase transitions occur when some symmetry element appears in the system, so in our case we have $c(4\times4)_4$, $c(3\times3)_{4-1}$, $c(2\times2)$ orderings.

For the first-order phase transitions between $c(4\times4)_4$ and $c(3\times3)_{41}$ phases we have monitoring dependence of $p(\rho)$ for different values of temperature and chemical potential. The coexistence density distributions for $T = 500$ K and $\Delta = 30$ kJ/mol are shown in the Fig. 9. One notes an existence of two pronounced peaks with the same area under each of them corresponding to different phases for $\mu^* = 3.85 \pm 0.05$ kJ/mol. That means μ^* is the coexistence value of the chemical potential under above conditions. The coexisting densities of the two coexisting phases correspond to the mean densities under these two peaks. The same calculations were performed for the first-order phase transitions between $c(3\times3)_{41}$–$c(2\times2)$ phase. The coexistence density distributions for, $T = 400$ K, $\Delta = 30$ kJ/mol for $\mu^* = 12.00 \pm 0.05$ kJ/mol are shown in Fig. 10. In order to determine the critical μ^* for the different temperatures in case of second-order phase transition we have used both methods discussed in Section 4a, the extrapolation of the positions $\mu_c(L)$ of

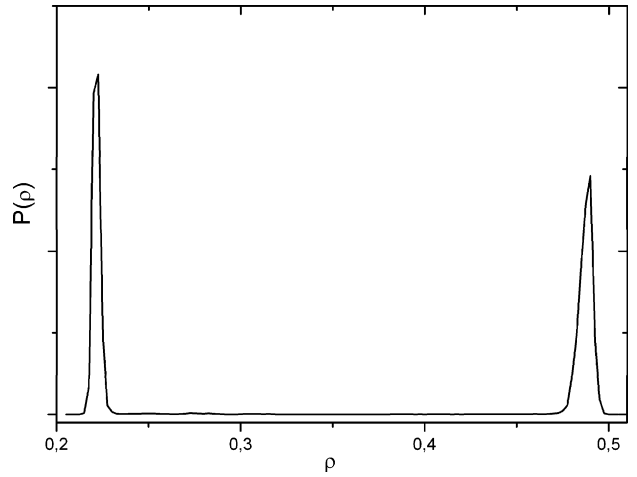

Fig. 10. Density distributions for $T = 400$, $\Delta = 30$ kJ/mol for coexistence value of chemical potential $\mu^* = 12.00 \pm 0.05$ kJ/mol at first-order phase transition $c(3\times3)_{4-1}$–$c(2\times2)$.

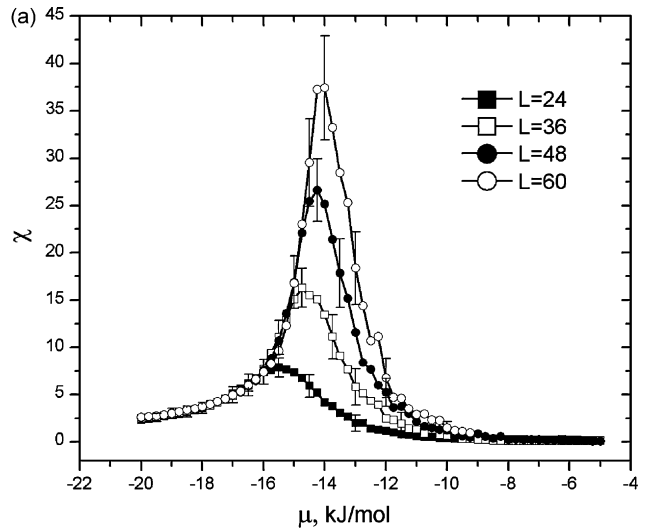

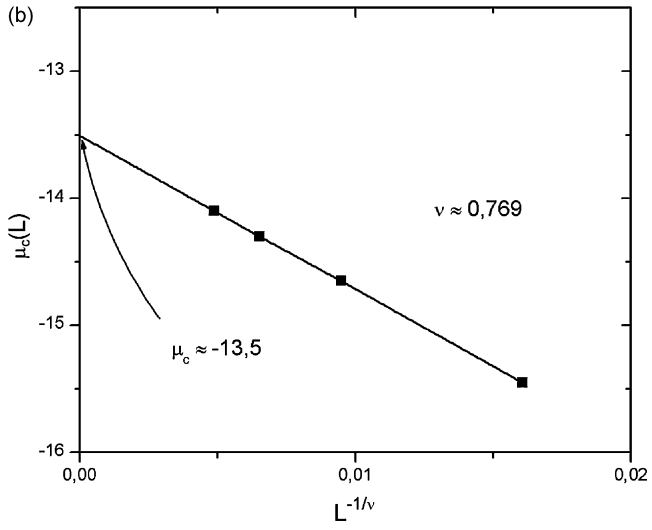

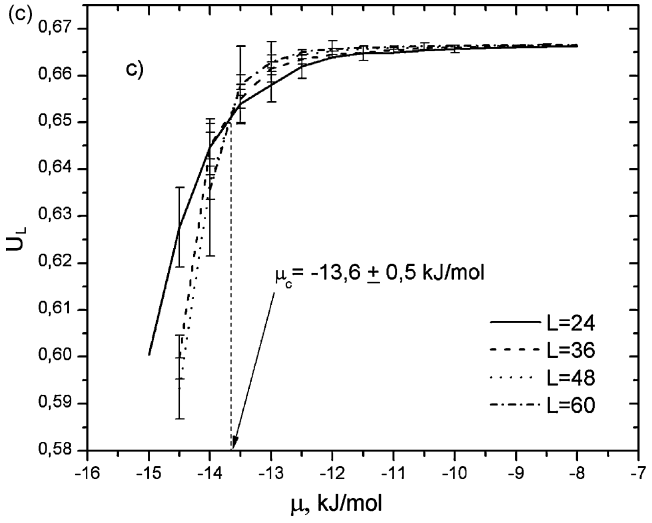

Fig. 11. Plots for estimation of second-order phase transitions at $\Delta = 30$ kJ/mol: (a) the $\chi(\mu)$ at $T = 400$, calculated for the different sizes of the lattice; (b) extrapolation of the maximum in susceptibility $\chi(\mu)_{max}$; (c) reduced four-order cumulants of the order parameter U_L versus μ for several lattice sizes.

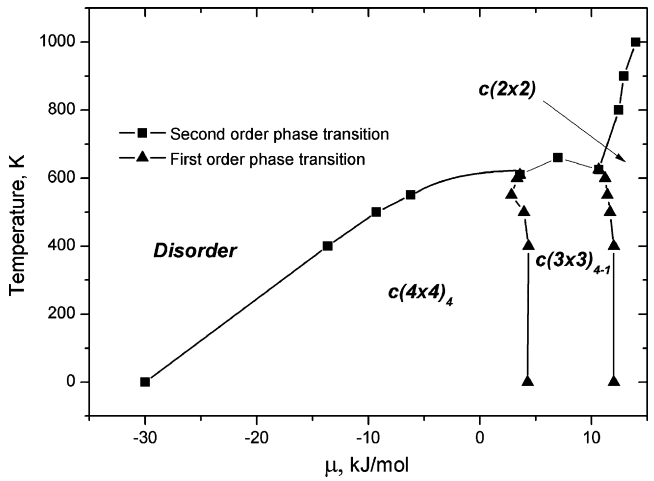

Fig. 12. The phase diagram of the model at $\Delta = 30$ kJ/mol.

susceptibility maxima $\chi(\mu)_{max}$ and the crossing in the cumulants. It should be mentioned that order parameter data were partly correlated, but it had not an essential effect on size of statistical errors, because the observation time was large enough. Fig. 11(a) shows the plot of the $\chi(\mu)$ at $T = 400$ K, $\Delta = 30$ kJ/mol calculated for the different sizes of the lattice.

From extrapolation of the maximum in susceptibility $\chi(\mu)_{max}$ as shown in Fig. 11(b) one can estimate the critical value of μ^* tuning the ν till all points $\chi(\mu)_{max}$ lay into the line. In Fig. 11(c) we have plotted the reduced four-order cumulants of the order parameter $U_L(\mu)$ versus μ for several lattice sizes. In vicinity of the critical point, cumulants have a strong dependence on the lattice size. However, at the critical point the cumulants tend toward the nontrivial value U^*_φ, irrespective of system size in scaling limit. Thus, plotting $U_L(\mu)$ for different lattice sizes yields an intersection point U^*_φ, which gives us sufficiently accurate estimation of the critical value of μ^* in the infinite system (Fig. 11(c)). Note that extrapolation of the maximum in susceptibility $\chi(\mu)_{max}$ gives a critical μ^* in agreement with that from the intersection of Binder's cumulants. In Fig. 12 we have presented the phase diagram of the adlayer consisting with complex molecules with different orientation for

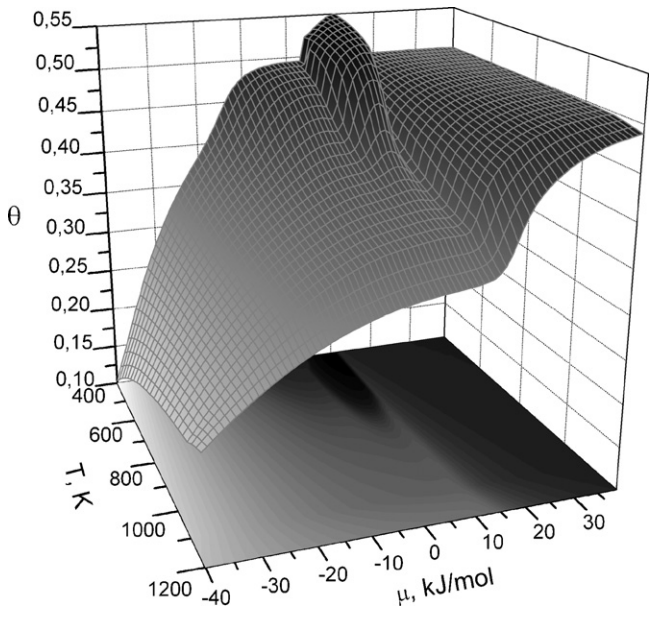

Fig. 13. Surface plot $\theta(\mu,T)$ calculated with transfer-matrix technique.

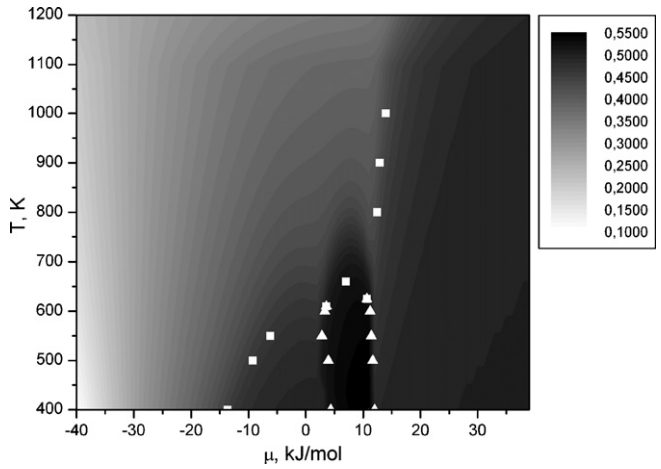

Fig. 14. The comparison of Monte Carlo simulation phase diagram (white symbols) with one estimated with transfer-matrix technique (surface plot). Scale of coverage is shown on the inset.

$\Delta = 30$ kJ/mol. There are three well-defined regions in the phase diagram corresponding to the order structures shown in Fig. 2. All appearing phases have chess-like symmetry, but: (i) $c(4\times4)_4$ phase consists of molecules with the same orientation in adlayer (adsorbed on four lattice sites); (ii) phase $c(3\times3)_{4-1}$ consists of molecules with different orientation in adlayer (adsorbed both on one and on four sites); (iii) $c(2\times2)$ appearing at higher pressure then others again consists of molecules with the same orientation in adlayer (but adsorbed on one lattice sites).

Additionally in the framework of the transfer-matrix method we calculated the set of surface coverage functions from chemical potential for different temperatures and stacked them into the surface plot $\theta(\mu, T)$ which corresponded to our phase diagram in (μ, T) coordinates calculated with Monte Carlo technique (Fig. 13).

In Fig. 14, we have shown the phase diagram obtained for the system under consideration with Monte Carlo simulation in comparison with $\theta(\mu,T)$ plot estimated by transfer-matrix technique. The qualitative agreement between both results is rather good.

6. Conclusion

In this paper we report an attempt to study general statistics of adlayers consisting with complex organic molecules on solid–gas interface. The effects of complex form of the adsorbing molecule, possibility of different orientation of the molecule in adlayer, multiple structure of the surface complexes have been investigated with Monte Carlo and transfer-matrix technique. Having investigated model under consideration we have found the surprising phenomenon. Namely, it has turned out that coverage dependence of chemical potential in the system can be nonmonotonic. That means, when pressure in gas phase increases the amount of empty adsorption sites increases too. Though an isotherm, as it follows from general thermodynamic lows, is monotonic increasing function. The reason for such phase behavior of the adlayer is the sequence of appearing phases, each of which is characterized by particular orientation of the adsorbing molecule in surface monolayer. Note, that existing of phases with different orientation of adsorbed molecules in adlayer is the experimentally confirmed fact.

Thus, we can do the following conclusions: the simplest model elaborated for SAMs shows rich phase diagram analogous to that for real SAMs; the structures of the model ordered phases are also analogous to the structures of SAMs; for SAMs the non-monotonous dependence of the total coverage on the pressure is possible, i.e. at the increase of pressure the empty surface area can grow that can take some effect on physicochemical processes on surface.

References

[1] C.B. France, F.A. Frame, B.A. Parkinson, Langmuir 22 (2006) 7507.
[2] Z. Li, B. Han, L.J. Wan, Th. Wandlowski, Langmuir 21 (2005) 6915.
[3] J.L. Ruggles, G.J. Foran, H. Tanida, H. Nagatani, Y. Jimira, I. Watanabe, I.R. Gentle, Langmuir 22 (2006) 681.
[4] O. Alexiadis, K.Ch. Daoulas, V.G. Mavrantzas, J. Phys. Chem. B 112 (2008) 1198.
[5] T. Yokoyama, S. Yokoyama, T. Kamikado, S. Mashiko, J. Chem. Phys. 115 (2001) 3814.
[6] H.S. Kato, M. Wakatsuchi, M. Kawai, J. Yoshinobu, J. Phys. Chem. C 111 (2007) 2557.
[7] W. Engel, L. Courbin, P. Panizza, Phys. Rev. B 70 (2004) (Art. No. 165407).
[8] W. Rżysko, M. Borówko, J. Chem. Phys. 117 (2002) 4526.
[9] F. Romá, A.J. Ramirez-Pastor, J.L. Riccardo, Langmuir 19 (2003) 6770.
[10] F. Romá, J.L. Riccardo, A.J. Ramirez-Pastor, Langmuir 22 (2006) 3192.
[11] W. Rżysko, M. Borówko, Phys. Rev. B 67 (2003) (Art. No. 045403).
[12] F. Romá, A.J. Ramirez-Pastor, J.L. Riccardo, Phys. Rev. B 68 (2003) (Art. No. 205407).
[13] T. Nitta, H. Kiriama, T. Shigeta, Langmuir 13 (1996) 903.
[14] W. Rżysko, A. Patrykiejew, K. Binder, Phys. Rev. B 72 (2005) (Art. No. 165416).
[15] V.F. Cabral, C.R.A. Abreu, M. Castier, F.W. Tavares, Langmuir 19 (2003) 1429.
[16] T. Schilling, S. Pronk, B. Mulder, D. Frenkel, Phys. Rev. E 71 (2005) (Art. No. 036138).
[17] M. Porto, H.E. Roman, Phys. Rev. E 62 (2000) 100.
[18] W. Rudziński, D.H. Everett, Adsorption of Gases on Heterogeneous Surfaces, Academic Press, London, 1992.
[19] V.P. Zhdanov, Elementary Physicochemical Processes on Solid Surfaces, Plenum Press, New York, 1991.
[20] A.V. Myshlyavtsev, G.S. Yablonskii, in: S.I. Kuchanov (Ed.), Mathematical Methods in Contemporary Chemistry, Gordon & Breach, New York, 1996.
[21] R.K. Baxter, Exactly Solved Models in Statistical Mechanics, Academic Press, London, 1982.
[22] L.K. Runnels, L.L. Combs, J. Chem. Phys. 45 (1966) 2482.
[23] P.A. Rikvold, J.B. Collins, G.D. Hansen, J.D. Gunton, Surf. Sci. 203 (1988) 500.
[24] A.V. Myshlyavtsev, V.P. Zhdanov, Chem. Phys. Lett. 162 (1989) 43.
[25] A.V. Myshlyavtsev, M.D. Dongak, J. Stat. Phys. 87 (1997) 593.
[26] A.V. Myshlyavtsev, M.D. Myshlyavtseva, Appl. Surf. Sci. 253 (2007) 5591.
[27] D.P. Landau, K. Binder, A Guide to Monte Carlo Simulation in Statistical Physics, Cambridge University Press, Cambridge, 2000.
[28] N. Metropolis, A.W. Rosenbluth, M.N. Rosenbluth, A.W. Teller, E. Teller, J. Chem. Phys. 21 (1953) 1087.
[29] K. Binder, D.P. Landau, Surf. Sci. 61 (1976) 577.
[30] K. Binder, Phys. Rev. Lett. 47 (1981) 693.
[31] A.M. Ferrenberg, R.H. Swendsen, Phys. Rev. Lett. 61 (1988) 2635.
[32] A.M. Ferrenberg, R.H. Swendsen, Phys. Rev. Lett. 63 (1989) 1195.
[33] J.J. de Pablo, Q. Yan, F.A. Escopedo, Annu. Rev. Phys. Chem. 50 (1999) 377.
[34] Q. Yan, J.J. de Pablo, J. Chem. Phys. 111 (1999) 9509.
[35] M.E.J. Newman, G.T. Barkema, Monte Carlo Methods in Statistical Physics, Oxford University Press, New York, 2001.